Single Particle Crushing under Slow Rate of Loading*

Saburo YASHIMA, Shoichi MOROHASHI** and Fumio SAITO

The Research Institute of Mineral Dressing and Metallurgy

(Received April 4, 1979)

Synopsis

An experimental study of the single particle crushing under a slow (constant) rate of loading was carried out by using specimens shaped into sphere made of quartz glass, borosilicate glass and six kinds of minerals. The diameters of sphere ranged from 0.5 to 3.0 cm and the rate of loading was fixed at 3 ton/min for the quartz glass and borosilicate glass specimens and 0.3 ton/min for the six kinds of minerals, respectively.

A summary of experimental results is as follows: 1) compressive strength of specimens was increased with the decrease of their volumes; 2) the status of fracture was mainly transcrystalline type; 3) in the case of hard material, experimental values of strain energy agreed fairly well with the theoretical values; 4) the strain energy was proportional to $\left(1-\frac{5}{3m}\right)$ power of volume of specimen, where "m" is the Weibull's coefficient of uniformity; 5) in coarse size range, the energy rule of single particle crushing was followed approximately by the Rittinger's law; 6) the reciprocal of size modulus of fractured products was proportional to (5/3) power of the compressive strength of specimen; 7) after obtaining the required energy where the crushing is made by a mill of industrial scale by applying the values of work index, the percentage of the strain energy at the time of fracture of a single spherical particle to the required energy was found 2.71 to 42.0 percent.

I. Introduction

Regarding the advancement of study on the comminution or crushing several courses can be conceived. In these investigations, it may be preferable to deal with the mechanism of crushing machine independent of the mechanism of single particle crushing within the crushing machine(1). Gilvarry(2) has tried the development of theory of the single particle crushing, and Bergstrom *et al.*(3). reported a number of related experimental results. Gilvarry's theory, assuming the latent crack distribution pre-existed in a solid particle, has derived a size distribution function and gave the theoretical interpretation of the R-R size distribution function and G-S as well. Bergstrom *et al.* studied mainly the relationship between fractured products and fracture energy of the single particle crushing.

Reviewing the methodology of studies of the mechanism of the single particle

---

* The **310th** report of the Research Institute of Mineral Dressing and Metallurgy. Reported in Japanese in Kagaku Kogaku, **34** (1970), 210.

** Department of Chemical Engineering, Faculty of Engineering, Toyama University, Toyama, Japan.

(1) T. Tanaka: The Micromeritics (Funsai), No. 3 (1968), 1.

(2) J.J. Gilvarry: J. Appl. Phys., **32** (1961), 400.

(3) B.H. Bergstrom, C.L. Sollenberger & W. Mitchell: Trans. A.I.M.E., **220** (1961), 367.

crushing, it is an operation to produce powder or to increase surface area by comminuting the given solid material. Accordingly, comminution is closely related to the learning of the material dynamics, as it is concerned the Young's modulus and Poisson's ratio inherent to the samples, the comminution is highly related to the rock mechanics. Furthermore, as comminution is an operation to break a solid in binding state into numerous pieces having fractured surface, it is preferred to observe the status mineralogically.

From the above mentioned point of view, since 1964, the authors have investigated such themes as fracture strength, fracture energy accumulated in the specimen, status of fracture and related themes regarding the single particle crushing of several kinds of glassy material and mineral. The present paper reports the experimental results concerning these subjects.

II. Samples

Eight different samples of glassy material and mineral, i.e., quartz glass, borosilicate glass, quartz, feldspar, limestone, marble, gypsum and talc, were used. Table 1 shows the density, Moh's hardness, Bond's work index obtained following the standard ball mill method[4], Young's modulus and Poisson's ratio of the samples by kind.

Table 1. Properties of samples

Kind of sample	Density ρ [g/cm^3]	Mohs' hardness H [−]	Work index W_i [kWh/ton]	Young's modulus Y_1 [Kg/cm^2]	Poisson's ratio ν_1 [−]
Quartz glass	2.20	6.5	14.8	$7.2_4\times10^5$	0.16
Borosilicate glass	2.33	6.5	15.2	$6.2_4\times10^5$	0.21
Quartz	2.62	6.5	13.3	$8.8_9\times10^5$	0.16
Feldspar	2.55	6.0	12.4	$5.9_9\times10^5$	0.26
Lime stone	2.70	4.0	9.40	$6.0_0\times10^5$	0.35
Marble	2.70	3.0	6.90	$5.4_5\times10^5$	0.30
Gypsum	2.30	2.0	6.30	$3.9_6\times10^5$	0.34
Talc	2.78	1.0	11.8	$1.5_3\times10^5$	0.33

The spherical specimens of glassy materials made by subcontracting to a glass maker, of which diameters "d" were sized carefully to within the range of 0.5 to 3.0 cm. The diameters "d" of the rod specimens were sized within 2.0 to 3.0 cm for quartz glass and within 0.5 to 3.0 cm for borosilicate glass. The ratio of "d" to the length of rod specimen "l" of these glassy specimens was made $d/l=1/2$. The quartz glass and borosilicate glass specimens were made following the annealing process so that the residual strain in the specimen is eliminated.

Regarding the mineral samples, these were cut and ground by using of a diamond saw and a grinder. Finally, these were finished into spherical specimens

(4) Mineral Dressing Committee: J. Min. Inst., Japan, **80** (1964), 293.

having diameters of 0.5 to 2.5 cm and the rod specimens having the same size with that of the glassy specimens by polishing using a grinding wheel with abrasive. The purities of these minerals were checked by X-ray analysis and chemical analysis, and the result indicated to be of high. The mineral specimens thus prepared were washed with distilled water and air-dried, and then held in a desiccator. In order to attain the confidence interval of the experimental results at a 95% level in a statistical sense, specimens of at least 20 were prepared by following the same method as that adopted by Yamaguchi[5]. The size and the number of the spherical specimens thus prepared are tabulated in Table 2. The finest particle size of the carborundum, which is used as the abrasive for polishing

Table 2. Nominal diameters and number of prepared specimens

Nominal diameter d [cm]	Quartz glass	Borosilicate glass	Quartz	Feldspar	Lime-stone	Marble	Gypsum	Talc
0.5	20	20	20	—	20	20	—	—
1.0	20	20	20	20	20	20	20	20
1.5	20	20	20	20	20	20	20	20
2.0	—	20	20	20	20	20	20	20
2.5	30	100	20	—	—	120	20	20
3.0	—	20	—	—	—	—	—	20

the total 900

purposes, was about 9μ. In the crushing tests of spherical and rod specimens, a pair of disks of loading platens mounted on the testing machine was made of tungsten carbide, and the surface roughness of the platens was finished to 1/100 mm. In the crushing tests of the rod specimens, a suspension of MoS_2 was spread on the upper and lower surfaces of a rod specimen in order to minimize the friction between the two platens. The tolerances for the nominal diameters of spherical specimens were finished within$\pm$0.7% relative for the glassy specimens and within $\pm$0.5% relative for the mineral specimens to the average of ten points of measurements. The values of compressive strength, Young's modulus and Poisson's ratio were obtained from the compression test of rod specimens. The surfaces roughness of the two surfaces of rod specimens was finished within $\pm$ 20μ. The tolerances for the nominal dimentions of rod specimens were finished within $\pm$ 0.25% relative and within $\pm$ 0.05% relative of the nominal length to the average of ten points of measurements.

III. Experimental apparatus

The compressive tester used for the experiment is a universal testing machine. (capacity 30 tons, range of loading rate 0.06–30 ton/min and sensitivity 5×10^{-4} ton) Load pacer is mounted on this testing machine in order to keep the loading at

(5) U. Yamaguchi: J. Soc. Mater. Sci., Japan, **14** (1965), 198.

a pre-set constant rate. The deformation of specimens for the loading direction was measured by differential transformers, and load and deformation were recorded by a X-Y plotter. Assembly of experimental apparatus (specimen, platens and differential transformers) is shown in Fig. 1. The Young's modulus and Poisson's ratio of the specimens, which were measured by using a cross wire strain gage mounted on the central portion of the loading direction to the specimen, were read from the load-deformation curves obtained by the load cell and the dynamic strain meter.

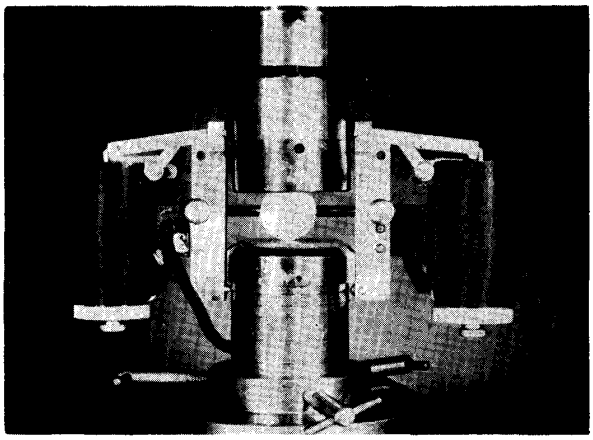

Fig. 1. Assembly of crushing apparatus (specimen, platens and differential transformers)

In size analysis of the fractured products, Tyler standard sieves ($2^{1/4}$ and $2^{1/2}$ series) were used. Particle size coarser than 3.5 mesh was represented by the average size of tri-axial dimensions of particle in relation to the aperture size of test sieve. Sieve shaker used was a Ro-tap type. Particle size and mass of the specimen were measured using a vernier caliper, micrometer and chemical balance.

IV. Experimental method

The specimen together with platens were placed in an acryle pipe holder so that the fractured products can be recovered completely. In order to prevent the scattering of fractured fragments of borosilicate glass specimen at a high speed and to prevent the secondary fracture at the wall of holder, the specimen was enclosed in the Japanese gelatin. Fractured products were recovered by washing out the Japanese gelatin several times with hot water. The maximum fracture load reached was measured by the load meter of the universal testing machine, and the strain energy accumulated in the specimen was read from the load-deformation curve. The Young's modulus of samples was obtained as the secant modulus of elasticity read from the stress-strain curve, and the Poisson's ratio was calculated from the values of longitudinal and lateral strains recorded by the X-Y plotter. The room temperature were 13 to 14°C throughout the period of experiments.

V. Experimental results and discussion

V–1. Effects of loading rate

In order to investigate the effects of loading rate upon the strain energy and sphere compressive strength, compression tests under various loading rates (0.06–30 ton/min) were carried out by using sphere specimens of 2.5 cm in diameter made of borosilicate glass and marble. These results are shown in Fig. 2. Strain energy and sphere compressive strength showed a tendency to increase with the increase of

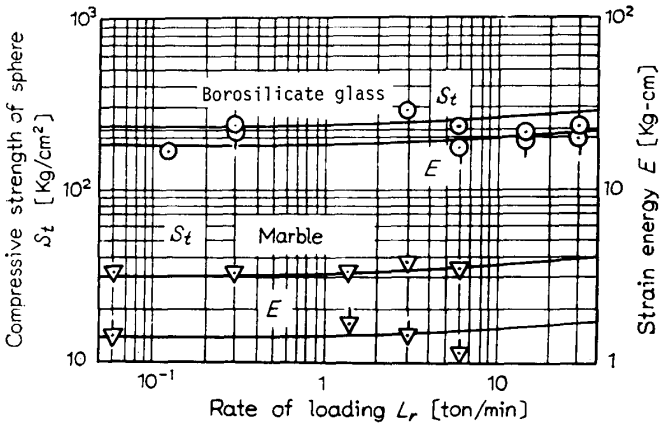

Fig. 2. Effects of rate of loading on strength and strain energy of sphere under compression

loading rate, however because of minor variations throughout all the procedures of experiment, the loading rate was set at 3 ton/min for borosilicate glass and quartz glass specimens and 0.3 ton/min for five kinds of mineral specimens.

V–2. Status of fracture in single particle crushing

Status of fracture in the single particle crushing is quite interesting. This status is detected by kinds of specimen as given below.

a) Borosilicate glass

The core of sphere, where the axis of the two loading points passes, are fractured into fine particles and surrounding portions to the core are broken into several crescent-shaped fragments. Status of fractured products of quartz glass sphere is similar to that of borosilicate glass as shown in Fig. 3. (a). (Gilvarry proved his own theory by similar experimental results.)

b) Quartz

Sphere of 2.0 cm in diameter consists of 4 to 5 crystal grains. Large fractured fragments of 3 to 4 pieces and a small number of fine fractured fragments are produced as shown in Fig. 3. (b)

c) Feldspar

Sphere of 2.0 cm in diameter is a single crystal. Status of fracture of

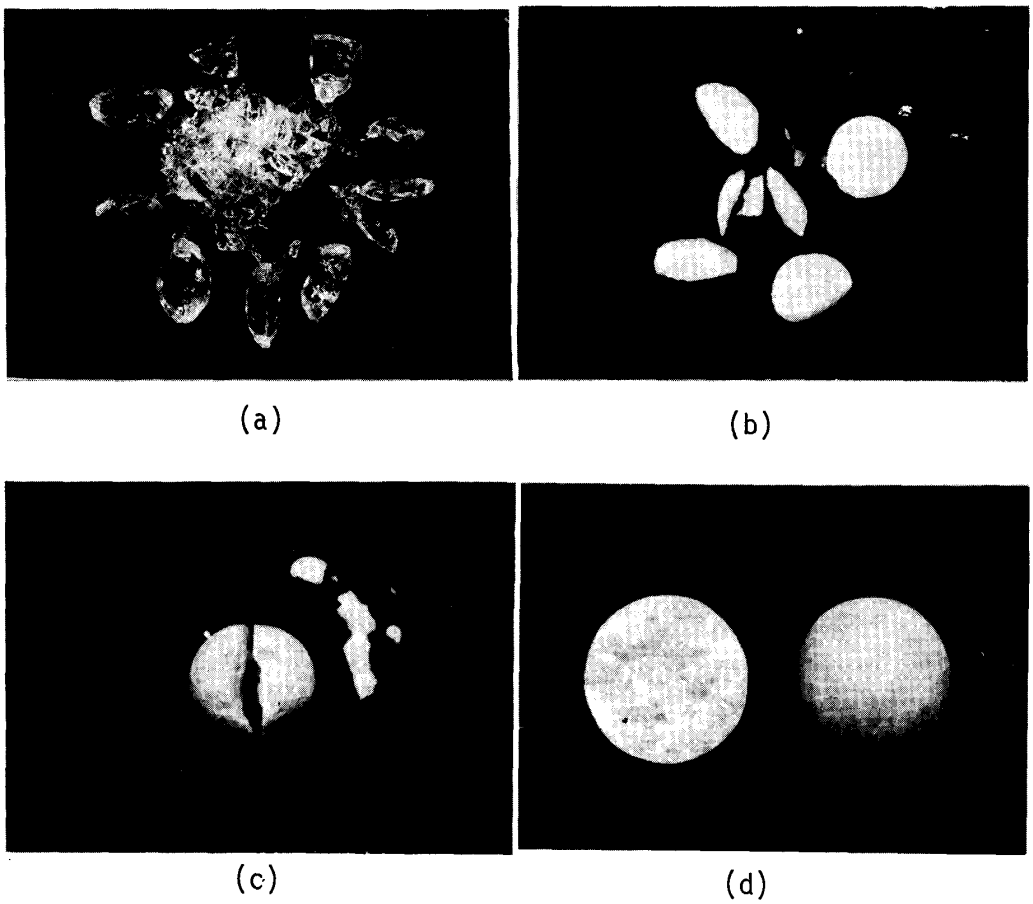

Fig. 3. Fragments of fractured specimen, (a) borosilicate glass, (b) quartz, (c) feldspar and (d) marble

feldspar is similar to that of quartz as shown in Fig. 3. (c).

d) Marble

Polycrystal. Crystal grain size is observable by naked eyes. Specimens are fractured into two semispheres at the great circle crosssection passing through the upper and lower loading points, as shown in Fig. 3. (d).

e) Limestone

Polycrystal. Crystal grain size is observable by naked eyes, but crystal grain size of this sample is smaller than that of marble. Fractured products separated into two portions were the same status as that of marble.

f) Gypsum

Polycrystal. Crystal grain size is microscopic. Status of fracture of this sample is similar to that of marble, whether or not the specimen is fractured is recognized with the crack generated on the surface of the specimen. Status of fracture of the talc specimen is similar to that of marble and gypsum specimens.

V–3. Status of fractured surface

Fractured fragments are fixed with Canadabalsam and the prepared specimens

having vertical plane to the fractured surface are prepared. The relationship between fractured surface and boundary of crystal grain is examined under a microscope. These results are as given below.

a) Quartz

Non cleavage fracture type. The condition of fractured surface is irregular as shown in Fig. 4. (a).

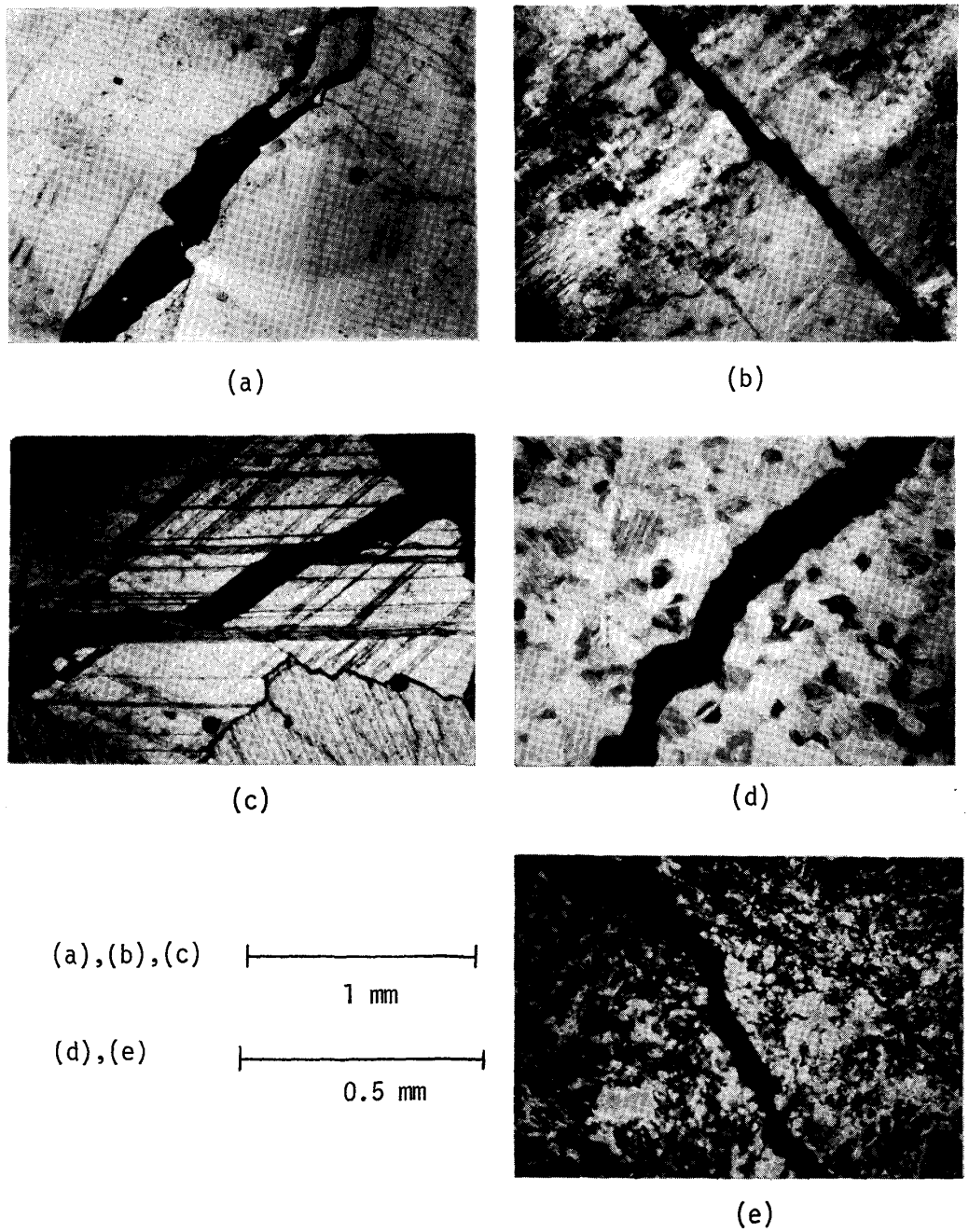

Fig. 4. Status of rectangular section of fractured surface, (a) quartz, (b) feldspar, (c) marble, (d) limestone and (e) gypsum

b) Feldspar

Cleavage fracture type. Fractured surface is plane along with the plane of cleavage as shown in Fig. 4. (b).

c) Marble

Cleavage fracture type. Fractured surface is plane along with the plane of cleavage, independent of boundary of crystal grain. The type of fracture is transcrystalline as shown in Fig. 4. (c).

d) Limestone

Cleavage fracture type. The type of fracture is transcrystalline, same as marble as shown in Fig. 4. (d).

e) Gypsum

Cleavage fracture type. Fine crystal structure. It seems that the types of fracture are transcrystalline and inter-crystalline as shown in Fig. 4. (e).

V–4. Size distribution of fractured products

The results of size analysis of fractured fragments of the spherical specimens represented by G-S distribution are shown in Figs. 5 and 6. The slope of the

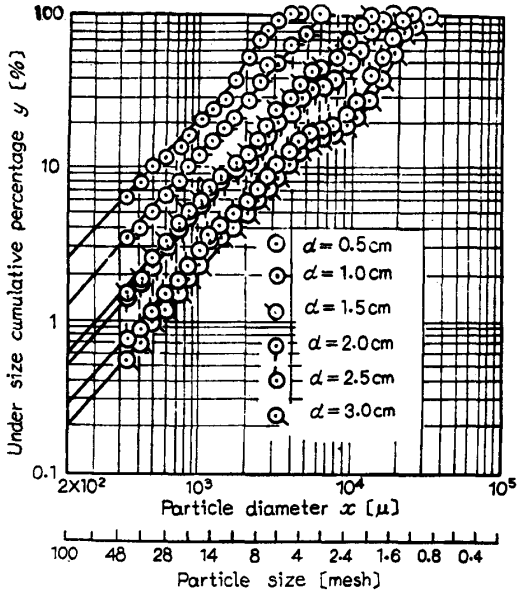

Fig. 5.

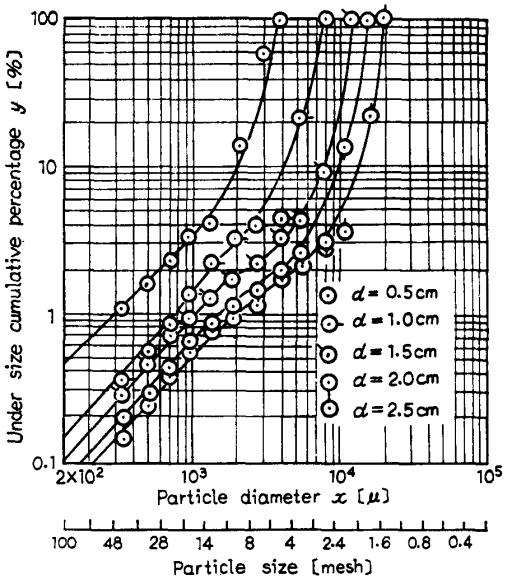

Fig. 6.

Fig. 5. Size distributions of fractured sphere of borosilicate glass
Fig. 6. Size distributions of fractured sphere of quartz

straight line on the part of fine particle range of borosilicate glass shown in Fig. 5 is nearly equal to unity, and in the case of quartz, the length of linear part of the regression line is shorter than that of borosilicate glass. The shape of the distribution curves of quartz glass is similar to that of borosilicate glass, and that of feldspar is similar to that of quartz. The percentage of finest undersize of minus 295 μ

of fractured products of sphere of 2.5 cm in diameter is 1.1% for quartz glass, 0.65% for borosilicate glass, 0.10% for quartz and in the case of sphere of feldspar having diameter of 2.0 cm, the percentage is 0.10%. As the specimens of marble, limestone, gypsum and talc have separated into semispheres at the fracture, and as the size of fractured products is defined by the maximum diameter, there are no changes in size before and after the fracture, under the size analysis by sieving.

V–5. Volume dependency of sphere compressive strength

The stress analysis by the point application of compressive load on spherical specimens has been conducted by Hiramatsu *et al.*(6). They showed that, as illustrated in Fig. 7, the tensile strength St is given by

$$St = 0.7P/\pi r^2 , \tag{1}$$

where P is the fracture load and r is one half of the distance between two loading points. Eq. (1) does not give the real tensile strength in its strict meaning, and, therefore, in this study St is called particle compressive strength. On the other hand, Weibull(7) carried out the study of brittle fracture of steel products at a low temperature, and showed the relationship between tensile strength St and volume of specimen V as given by

$$St \propto V^{-1/m} , \tag{2}$$

where m is the coefficient of uniformity. Eq. (2) designates that the tensile strength decreases with the increase of volume of specimen. For the brittle

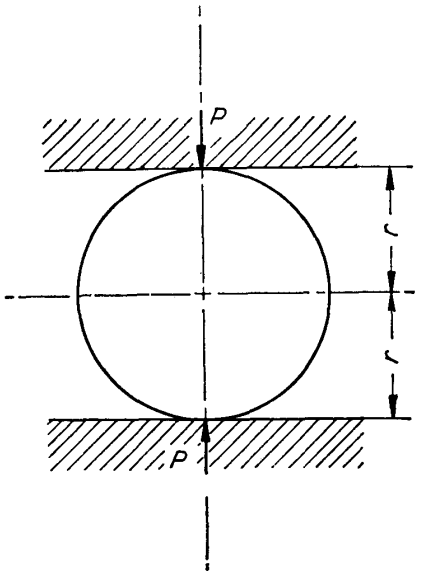

Fig. 7.

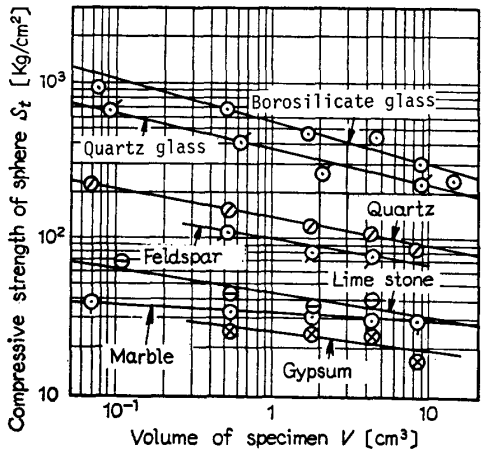

Fig. 8.

Fig. 7. Compression of sphere
Fig. 8. Volume dependency of compressive strength of various specimens

(6) Y. Hiramatsu, T. Oka, H. Kiyama: J. Min. Inst., Japan, **81** (1965), 1024.
(7) W. Weibull: J. Appl. Phys., **18** (1951), 293.

materials used in the present study, as shown in Fig. 8, it is confirmed that the relationship between St and V can be expressed by the Weibull's equation. The value of "m" is determined by the reciprocal of gradient of straight line as reported by Davidenkov[8]. On the other hand, the method of determining the value of "m" advocated by Ueno[9] is that method to obtain St^* from the dispersion of measurements. The values of coefficient of uniformity "m" is calculated by the method of least squares from the gradient of straight lines (see Fig. 8), and the values of "m" is calculated from Eq. (3) using experimental data. These are presented on Table 3; both values agree well in the range of experiments.

Table 3. Coefficient of uniformity

Kind of sample	Calculated from gradient of straight lines of Fig. 8 by least squares method m [−]	Calculated from Eq. (3) using experimented value of specimens m [−]
Quartz glass	4.75	4.38
Borosilicate glass	4.27	3.48
Quartz	5.10	4.86
Feldspar	4.70	3.73
Lime stone	7.59	6.10
Marble	19.0	—
Gypsum	0.72	—
Talc	—	—

V–6. Strain energy in single particle crushing

As the strain energy in the single particle crushing is the energy accumulated in the specimen until the specimen is fractured, it is a quite important value related to the net energy in comminution. When a sphere of elastic material is subject to loading between two platens as illustrated in Fig. 7, the strain energy accumulated in a sphere is given by Eq. (4) which is derived after the Timoshenko's theory**.

(8) N. Davidenkov, E. Shevandin & F. Wittman: J. Appl. Mech., **14** (1947), A-63.

(9) G. Ueno: J. Soc. Mater. Sci., Japan, **9** (1960), 21.

* From the histogram of tensile strength measured by using a number of specimens, Ueno has advocated that the value of coefficient of uniformity is able to calculate by

$$c = \sigma/\mu = \left[\Gamma\left(1+\frac{2}{m}\right)\Big/\left\{\Gamma\left(1+\frac{1}{m}\right)\right\}^2 - 1\right]^{1/2}, \tag{3}$$

Where σ is the standard deviation, μ the mean value and "c" the coefficient of variation.

** Derivation of theoretical equations as applied to the compression of sphere placed between two parallel platens, as shown in Fig. 7, reported by Timoshenko[10] on the basis of Hertz's theory is made available in the literature 3).

The solution is

$$E = (4/5)(3/4)^{5/9}\left(\frac{1-\nu_1^2}{Y_1} + \frac{1-\nu_2^2}{Y_2}\right)^{2/3}\left(\frac{\pi}{V}\right)^{1/9} P^{5/3}, \tag{4}'$$

consequently

$$E = 0.682\left(\frac{1-\nu_1^2}{Y_1} + \frac{1-\nu_2^2}{Y_2}\right)^{2/3}\left(\frac{\pi}{V}\right)^{1/9} P^{5/3}. \tag{4}$$

$$E = 0.682\left(\frac{1-\nu_1^2}{Y_1} + \frac{1-\nu_2^2}{Y_2}\right)^{2/3}\left(\frac{\pi}{V}\right)^{1/9} P^{5/3}, \qquad (4)$$

where ν_1 is the Poisson's ratio, Y_1 the Young's modulus of samples and Y_2 the Young's modulus of platens made of tungsten carbide. Suffixes 1 and 2 designate the sample and platens, respectively, and $Y_2=6.05\times10^6$ Kg/cm^2 and $\nu_2=0.21$ for the present experiment. Measured values of Young's modulus and Poisson's ratio of various samples are tabulated in Table 1. An example of the load-deformation curve for the compression of sphere is shown in Fig. 9. The area embraced between the load-deformation curve and the abscissa represents the strain energy. On the

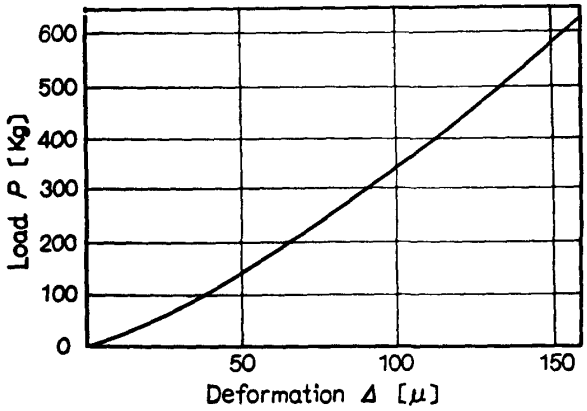

Fig. 9. Load-deformation curve of sphere of feldspar

other hand, when the experimental data of the Young's modulus Y_1, Poisson's ratio ν_1 and fracture load P are placed in Eq. (4), calculated value of strain energy can be obtainable. Comparison of experimented values and calculated values of the strain energy in the sphere compression tests of quartz and marble is shown in Fig. 10. The experimented values agree quite well with the calculated values in quartz

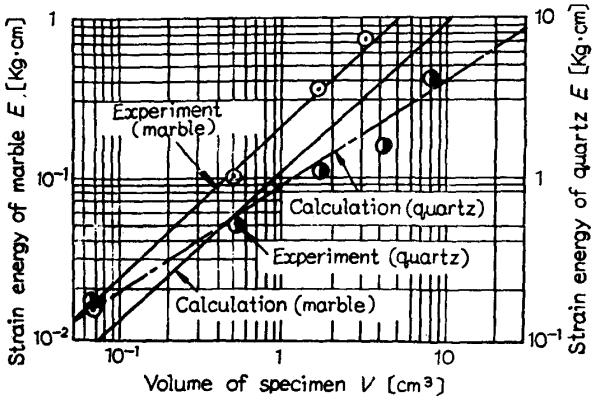

Fig. 10. Comparison of experimented value and calculated value of strain energy on compression of sphere of quartz and marble

glass, borosilicate glass, quartz and feldspar, but in marble, the experimented values are larger than that calculated. Of the soft materials such as marble, the flow of

structure occured in the neighborhood of the loading points and part of the strain energy is converted into plastic deformation energy, where as the Young's modulus used in Eq. (4) is a large value measured at the initial state of application of compressive load. Of the samples softer than marble used in the present experiment, plastic deformation occured during the fracture process. Status of stress distribution observed in marble specimen is shown in Fig. 11. It seems that the stripe pattern observed in Fig. 11 is the stress distribution causes by compressive

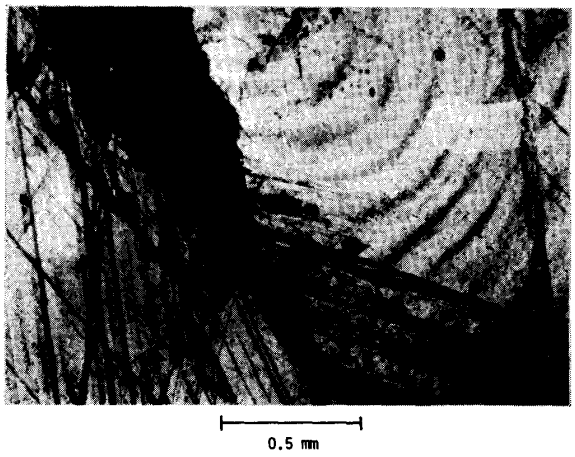

Fig. 11. Status of stress distribution observed in marble specimen

load in the neighborhood of loading points of spherical specimen, and it may be the same phenomenon as the photo elasticity. But, such pattern as observed in Fig. 11 is not observed in quartz and feldspar.

V–7. Volume dependency of strain energy in single particle crushing

Volume dependency of strain energy in the single particle crushing is examined. Eq. (2) is modified by introducing a constant C_1.

$$St = C_1 V^{-1/m} . \tag{5}$$

From Eqs. (1), (4) and (5), we obtain

$$\left.\begin{aligned} E &= C_2 V^{(1-\frac{5}{3m})} \\ \text{where} \quad C_2 &= 0.898\left(\frac{1-\nu_1^2}{Y_1}+\frac{1-\nu_2^2}{Y_2}\right)^{2/3} \pi^{2/3} C_1^{5/3} . \end{aligned}\right\} \tag{6}$$

Volume dependency of strain energy of borosilicate glass and quartz spheres are shown in Fig. 12. The relationship between strain energy and volume of specimen on the logarithmic coordinate was able to express by a straight line having the gradient of $\left(1-\frac{5}{3m}\right)$. The solid line and the chain dotted line in Fig. 12 are those calculated from Eq. (6). Both of them were in good agreement with the experimental results. From the present experiment, we can calculate the fracture energy from Eq. (6) by measuring the coefficient of uniformity.

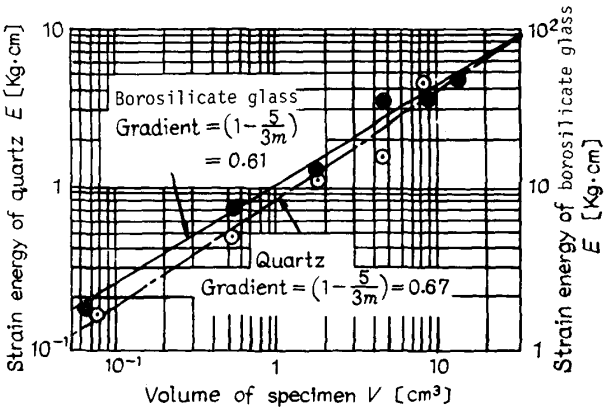

Fig. 12. Volume dependency of strain energy of borosilicate glass and quartz sphere

V–8. Applicability of the two laws in single particle crushing

This clause covers the investigation of applicability of the two laws called Rittinger's law and Kick's law respectively from the following three methods (1), (2) and (3) to the present experiment concerning the single particle crushing under a slow (constant) rate of loading in coarse size range of materials.

(1) Method of determination from an index of Lewis' general equation

Lewis'[11] general equation expressed by the relationship between fracture energy and particle size is given by

$$d\left(\frac{E}{M}\right) = -C_3 \frac{1}{x^n}\, dx\,, \tag{7}$$

where E is the fracture energy, M the mass of specimen, x the particle size, C_3 the constant and "n" the index. Eq. (8) is obtained by integrating Eq. (7).

$$\frac{E}{M} = \frac{C_3}{n-1}\,\frac{1}{x^{n-1}} \tag{8}$$

It is determined by the value of "n" in Eq. (8) as to which of the two laws can be applied to the single particle crushing. On the other hand, from size distribution curves of fractured fragments of borosilicate glass and quartz spheres shown in Figs. 5 and 6, the relationship between passing size x at a given undersize cumulative mass percentage and specific fracture energy (E/M) is plotted on the logarithmic coordinate, and the results are given in Figs. 13 and 14. In these two figures the passing size x is inversely proportional to the specific fracture energy. When the gradient of this straight line is denoted by "a" and the intercept of this straight line by xa, we obtain

$$E/M = (1/xa)^{1/a}\,(1/x^{-1/a}) \tag{9}$$

Comparing the index of x in Eq. (8) with that in Eq. (9) we have

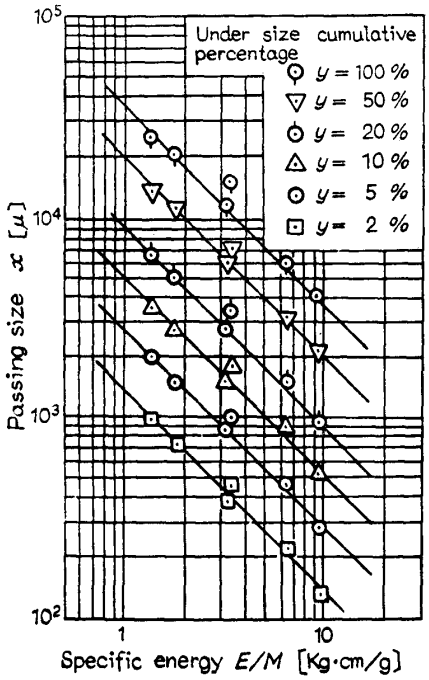

Fig. 13.

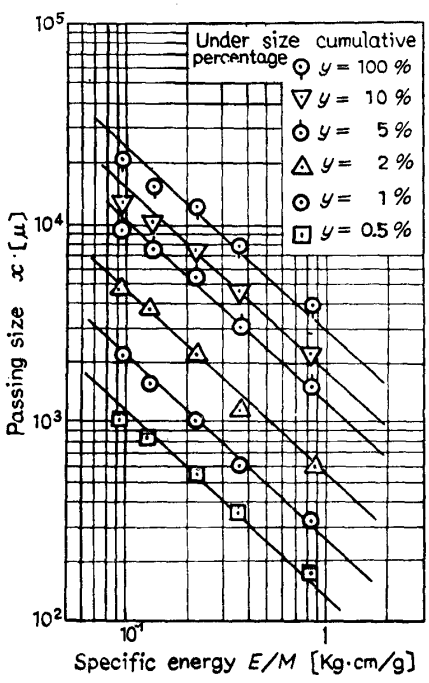

Fig. 14.

Fig. 13. Relation between specific energy and passing size of borosilicate glass sphere
Fig. 14. Relation between specific energy and passing size of quartz sphere

$$n = 1 - \frac{1}{a} . \tag{10}$$

The value of index "n" in Lewis' general equation is determined by the gradient of straight line "a". For example, the determined values are as follows; n=2.0 at a=−1.0 for borosilicate glass sphere; n=2.1 at a=−1.9 for quartz sphere; n=2.2 at a=−0.8 for feldspar sphere; and n=1.9 at a=−1.1 for quartz glass. In the single particle crushing under a slow constant rate of loading, in a coarse size range of borosilicate glass, the Rittinger's energy law is possible to apply exactly, and this law is applicable approximately to quartz, feldspar and quartz glass. When the value of index "n" is above 2, it means that the specimen include the latent surface which will become new surface before the specimen is fractured. When the value of index "n" takes the value between 1 and 2, it seems that the fracture process of part of the specimen follows the Rittinger's energy law and the fracture process of the other part of specimen follows the Kick's energy law.

(2) *Method of determination from the incremental increases of specific surface area*

If the Rittinger's energy law is applied to the single particle crushing, we have

$$E/M = C_4(S - S_0) = C_5(1/x - 1/x_0) , \tag{11}$$

where x_0 is the corresponding diameter to specific surface area of specimen, x the related diameter to specific surface area of fractured products, S_0 the specific surface area of specimen, S the specific surface area of fractured products, and C_4

and C_5 the constants. For example, the relationship between (E/M) and $(1/x-1/x_0)$ concerning the borosilicate glass specimen is shown in Fig. 15. The relationship is able to express by a straight line, consequently, the Rittinger's energy law is found applicable to all kinds of sample covered by the present study.

(3) Method of determination from the modified G-S plotting

For example, from the G-S size distribution of fractured products of borosilicate glass specimen, at values $1/x$ (inverse of particle size x) on the abscissa, the relationship between $(1/x\text{-}1/x_0)$ and (E/M) on a logarithmic coordinate with parameter y of a given undersize cumulative mass percentage are as shown in Fig. 16. As can be seen from this figure, the straight line having gradient unity is obtained. From the above result, it is found that Eq. (11) can be validated and the Rittinger's energy law can be applicable as an approximation.

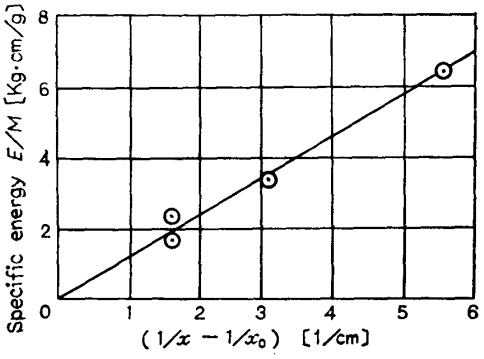

Fig. 15.

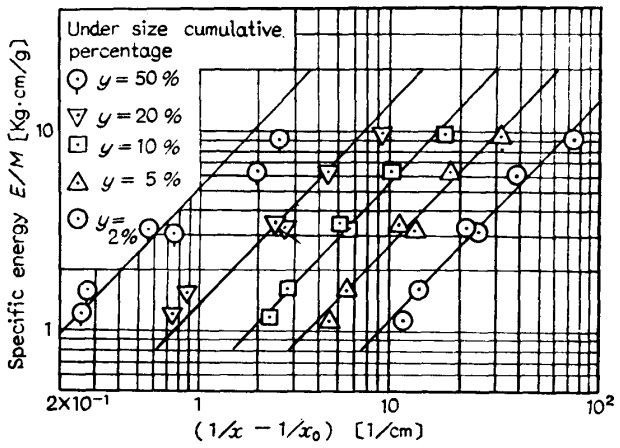

Fig. 16.

Fig. 15. Relation between $(1/x-1/x_0)$ and specific energy of borosilicate glass sphere
Fig. 16. Relation between $(1/x\text{-}1/x_0)$ and specific energy of borosilicate glass sphere

V–9. Relationships between strain energy, sphere compressive strength and particle size in single particle crushing

From the above results, it is found that the relationships between strain energy, sphere compressive strength and particle size in the single particle crushing in coarse size range under a slow constant rate of loading can be derived. From Eqs. (1) and (4), we obtain

$$\left.\begin{aligned} E/V &= C_6 S_t^{5/3} \\ \text{where} \quad C_6 &= 0.898\left(\frac{1-\nu_1^2}{Y_1}+\frac{1-\nu_2^2}{Y_2}\right)^{2/3}\pi^{2/3}. \end{aligned}\right\} \tag{12}$$

In the single particle crushing in a coarse size range, as the Rittinger's energy law can be applied, so by assuming $n=2$, then Eq. (7) becomes

$$d(E/M) = -C_3(1/x^2)\,dx\,. \tag{13}$$

By integrating Eq. (13) from $x_1=k_0$ [μ] of the size of sphere specimen to $x_2=k_{100}$ [μ] of the size modulus of fractured products, we obtain

$$(E/M) = C_3 \int_{k_0}^{k_{100}} (1/x_2)\, dx = C_3(1/k_{100} - 1/k_0)\,, \tag{14}$$

if $k_{100} \ll k_0$, Eq. (14) becomes

$$(E/M) = C_3(1/k_{100}) \tag{15}$$

It is found that the specific fracture energy varies inversely proportional to the size modulus k_{100} of fractured products. When the density of sample is denoted by ρ, as $M=\rho V$, so the following equation is derived from Eqs. (12) and (14):

$$\left.\begin{aligned} &1/k_{100} - 1/k_0 = C_7 S_t^{5/3} \\ &\text{where} \\ &C_7 = (0.682/C_3\rho)\left(\frac{1-\nu_1^2}{Y_1} + \frac{1-\nu_2^2}{Y_2}\right)^{2/3}. \end{aligned}\right\} \tag{16}$$

If $k_{100} \ll k_0$, Eq, (16) becomes

$$1/k_{100} = C_7 S_t^{5/3}\,. \tag{17}$$

In order to prove Eq. (12), (E/V) and St calculated from the experimental data are plotted on a logarithmic coordinate. As shown in Fig. 17, (E/V) is proportional to the power of 5/3 of St and it was proved that Eq. (12) can be applicable exactly to the experimental results. Fig. 18 is the result that experimentally scrutinized Eq. (14), and Fig. 19 is the result that experimentally scrutinized Eq. (16). As the gradient of each straight line becomes 5/3, it was proved that Eq. (16) can be applicable exactly to the experimental results.

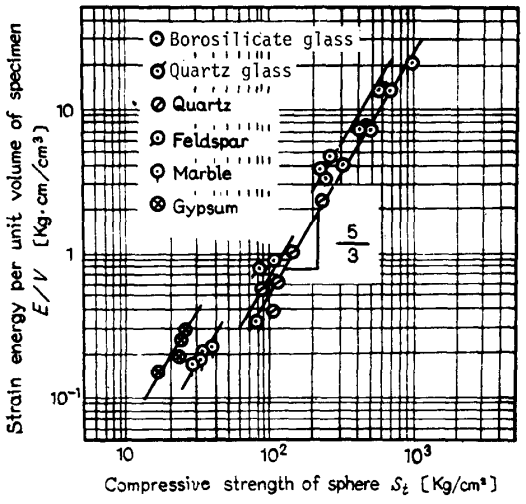

Fig. 17.

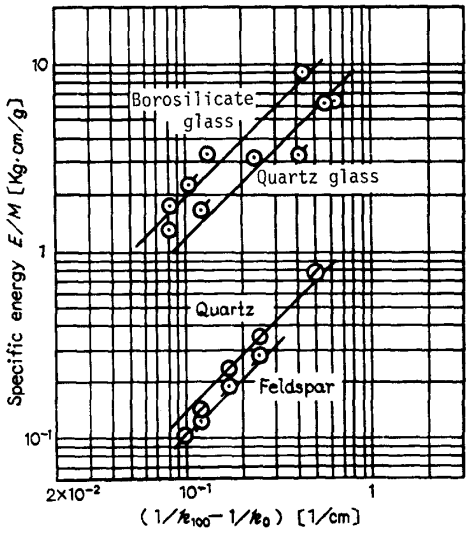

Fig. 18.

Fig. 17. Relation between compressive strength and strain energy per unit volume of specimen

Fig. 18. Relation between $(1/k_{100}-1/k_0)$ and specific energy

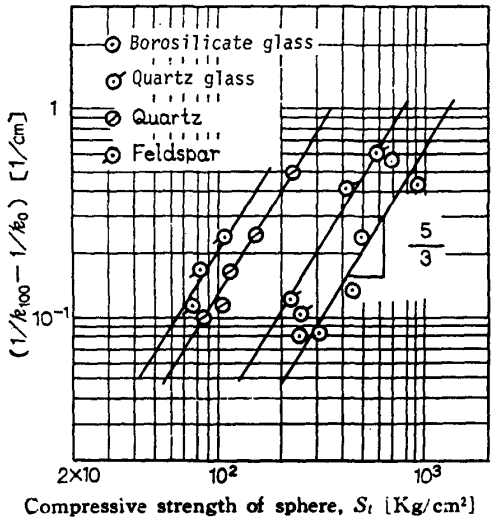

Fig. 19. Relation between $(1/k_{100}-1/k_0)$ and compressive strength of sphere

VI. Conclusion

Experiments concerning the single particle crushing under a slow constant rate of loading were carried out, and the following results were obtained:

(1) The strain energy and sphere compressive strength does not give a large effect upon the loading rate if it is a slow constant rate.

(2) From the mineralogically observed results of the fractured surfaces of crushed single particle, it became apparent that the fracture of mineral specimens having a cleavage structure is the transcrystalline type.

(3) The size distributions of fractured products in quartz glass, borosilicate glass, quartz, feldspar show a similar pattern (see Fig. 5 and Fig. 6). In the other samples, specimens are fractured into two semispheres bordering at the great circle passed through the axis between the upper and lower loading points.

(4) As the results of examination made on the volume dependency of sphere compressive strength concerning all kinds of sample involved, it was proved that they evidently follow the Weibull's relation.

(5) Comparing the experimented values and calculated values of strain energy in the single particle crushing, both values are in a tendency of good agreement for quartz glass, borosilicate glass, quartz and feldspar. On the other hand, experimented values are tended to be generally greater than the calculated values for marble, gypsum and talc.

(6) Investigating the volume dependency of strain energy in the single particle crushing, it was found that Eq. (6) can be applied exactly. Strain energy accumulated in a specimen until it is fractured can be obtained by measuring the coefficient of uniformity.

(7) Percentages of strain energy in the single particle crushing to the industrial scale mill energy obtained by using Bond's work index, assuming that the same crushing takes place by the industrial scale mill, are 41.7% for quartz glass, 42.0% for feldspar, 2.71% for marble, and 4.51% for gypsum. However at present,

percentage of energy consumed in the increases of new surface to the strain energy in the single particle crushing is not known.

(8) The Rittinger's energy law can be applied to the single particle crushing in a coarse size range under a slow constant rate of loading.

(9) Eqs. (12), (14) and (16) can be applied to the relationships between strain energy, sphere compressive strength and particle size in the single particle crushing under a slow constant rate of loading.

(10) As plastic deformation occurs in compression of talc sphere, it is necessary to explain this phenomenon from the rheological point of view.

(11) Previously, an experimental study on the single particle crushing used for several materials having high bonding force, such as pyrex glass and sapphire, was carried out by Gilvarry and Bergstrom *et al.* However, in the present study, it is found that the characteristics of fracture in minerals differed from that of the materials having high bonding forces.